Doping effects of hexagonal manganites $Er_{1-x}Y_xMnO_3$ with triangular spin structure

M. Chandra Sekhar,[1,2] Seongsu Lee,[1] Gwangho Choi,[1] Changhee Lee,[3] and J.-G. Park[1,2,*]
[1]*Department of Physics and Institute of Basic Sciences, SungKyunKwan University, 440-746 Suwon, Korea*
[2]*Center for Strongly Correlated Materials Research, Seoul National University, Seoul 151-747, Korea*
[3]*Neutron Physics Laboratory, Korea Atomic Energy Research Institute, Daejon 305-600, Korea*
(Received 2 November 2004; revised manuscript received 4 April 2005; published 1 July 2005)

We have studied doping effects of hexagonal manganites $Er_{1-x}Y_xMnO_3$, which are found to have 2D triangular spin structure for all the samples studied here. Upon doping Er at the Y site, the magnetic structure changes gradually from the Γ_1 representation of $YMnO_3$ to the Γ_2 representation of $ErMnO_3$ while the ordered moment remains almost unchanged in magnitude over the whole doping range. Despite the gradual change in the magnetic structure with doping, geometrical frustration effects expected of the 2D triangular spin structure with antiferromagnetic interaction between nearest neighbors show very strong doping dependence. For example, although $YMnO_3$ shows all the signs of Mn moments being geometrically frustrated in the susceptibility and neutron diffraction data, such evidence of frustration effects is nearly absent in $ErMnO_3$. We suggest that magnetic coupling along the *c* axis between Er and Mn moments should be responsible for the drastic doping dependence of the geometrical frustration effects.

DOI: 10.1103/PhysRevB.72.014402 PACS number(s): 75.50.Ee, 61.12.Ld, 75.40.Cx

I. INTRODUCTION

Rare-earth manganites $RMnO_3$ form in one of two crystal structures, orthorhombic and hexagonal phases, depending on the ionic size of rare-earth elements. The orthorhombic phase with space group *Pbnm* is found for R=La, Pr, Nd, Sm, Eu, Gd, Tb, and Dy with a large ionic radius[1] while the hexagonal phase with space group $P6_3cm$ is found for R=Ho, Er, Tm, Yb, Lu, Y, and Sc with a relatively smaller ionic radius.[2]

Recent revival of interest in the hexagonal manganites is largely due to the coexistence of both ferroelectric and antiferromagnetic transitions in these materials, the so-called multiferroic phenomenon. For example, $YMnO_3$ has antiferromagnetic transition temperature at T_N=70 K and, at the same time, ferroelectric transition temperature at T_C=913 K while $ErMnO_3$ has T_N=79 K and T_C=833 K.[3] Therefore, the hexagonal manganites provide a rare opportunity of exploring a possible coupling between the two order parameters and maybe even controlling one order parameter by another in the future.

Further interest arises from a unique magnetic structure found for these hexagonal manganites. In the crystal structure of the hexagonal $RMnO_3$, there are six formula units per unit cell and six Mn atoms are located on the z=0 and z=1/2 planes, respectively. According to several neutron diffraction studies,[4–7] the magnetic moments of Mn ions of $YMnO_3$ and $ErMnO_3$ lie on the *ab* plane and form an edge-sharing triangular magnetic structure. Because of this triangular magnetic structure, the antiferromagnetic ordering temperature of the hexagonal manganites is much suppressed when compared with their respective Curie-Weiss temperatures, θ_{CW}. For instance, $YMnO_3$ orders antiferromagnetically at T_N=70 K although it has a much larger Curie-Weiss temperature, θ_{CW}=−545 K. Therefore, the ratio of $f=|\theta_{CW}|/T_N$ is as large as 7.8 for $YMnO_3$, which makes it one of the so-called geometrically frustrated systems.[8] On the other hand, this frustration factor, f, is significantly reduced for $ErMnO_3$: with T_N=78 K and θ_{CW}=−81 K it is f=1.0. What is unique about the magnetic structure of the hexagonal manganites is that it is a rare example of 2D spin systems with an easy plane anisotropy. Another evidence of such frustration effects can also be found in neutron diffraction data that show the existence of short-range correlations well above the actual antiferromagnetic transition temperature.[9]

According to the theoretical analysis of possible magnetic structures for the hexagonal manganite using a magnetic group theory,[5] altogether six magnetic structures are found to be possible with k=0: two 1D representations with one component (Γ_1 and Γ_4) and another two 1D representations with two components (Γ_2 and Γ_3) and two 2D complex representations (Γ_5 and Γ_6). Until now, all hexagonal manganites are reported to have magnetic structures of either Γ_1/Γ_3 or Γ_2/Γ_4 representations. For example, $YMnO_3$ belongs to the former while $ErMnO_3$ belongs to the latter. We found that it is difficult to distinguish between the Γ_1 and Γ_3 representations within the resolutions of our neutron diffraction experiments of $YMnO_3$.[6] The same is true for the Γ_2 and Γ_4 representations of $ErMnO_3$.

For our later discussion, we describe the magnetic structure with the 1D representations in more detail. For the Γ_1 and Γ_4 representations, the magnetic moment of Mn (Mn1) at the $(x,0,0)$ position is aligned perpendicular to the [100] axis. Furthermore, the Γ_1 representation has an antiferromagnetic coupling between the moments at the z=0 and z=1/2 planes whereas for the Γ_4 representation the interplane coupling is of ferromagnetic nature. On the other hand, for the Γ_2 and Γ_3 representations, the in-plane magnetic moment of Mn1 is aligned parallel to the [100] axis. In addition, for the Γ_2 representation the in-plane moments are coupled antiferromagnetically along the *c* axis while the out-of-plane components are ferromagnetically coupled along the *c* axis. On the other hand, for the Γ_3 representation the in-plane components are coupled ferromagnetically along the *c* axis while the out-of-plane components are antiferromagnetically coupled along the *c* axis.

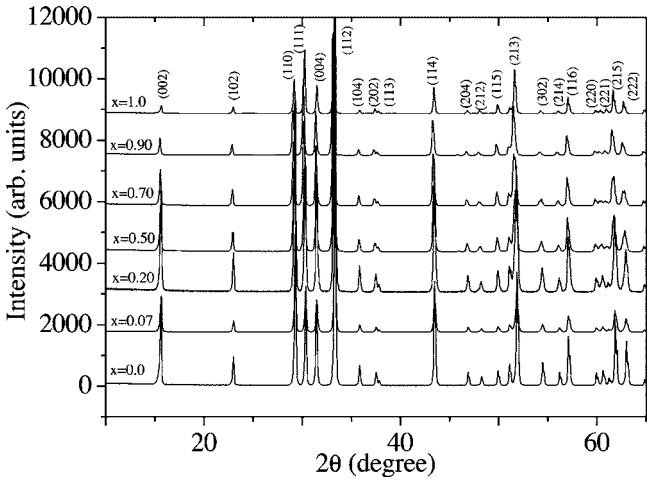

FIG. 1. The room temperature x-ray diffraction patterns are shown for a few representative samples of $Er_{1-x}Y_xMnO_3$ with x =0.0, 0.07, 0.20, 0.50, 0.70, 0.90, and 1.0 (from bottom to top). For better presentation, the data are shifted upward.

In this paper, we report doping effects on the frustration effects and the magnetic structure of (Y,Er)MnO_3. From this study, we found that Er moments play an important role in reducing the geometrical frustration of Mn moments, probably through magnetic interactions between the two layers of magnetic moments. We have also observed that even a small amount of doping induces mixing between the two magnetic structures of $YMnO_3$ and $ErMnO_3$.

II. EXPERIMENTAL DETAILS

We prepared 11 samples of $Er_{1-x}Y_xMnO_3$ (x=0.0, 0.03, 0.07, 0.10, 0.15, 0.20, 0.30, 0.50, 0.70, 0.90, and 1.0), using Y_2O_3, Er_2O_3, and Mn_2O_3 of 99.999% purity (AR grade) by a standard solid state reaction method. All the starting materials were mixed and ground several times in order to produce a homogeneous mixture. The final sintering was made at 1300 °C for 24 h with intermediate grinding. Subsequent XRD (x-ray diffraction) measurements using Cu $K\alpha$ (D/MAX-2200 Ultima, Rigaku) show no trace of impurities phases, and all the measured patterns can be indexed according to the $P6_3cm$ space group of the hexagonal manganites as shown in Fig. 1.

We measured magnetization using a commercial SQUID magnetometer (MPMS-5XL, Quantum Design) from 2 to 300 K and a vibrating sample magnetometer (Lakeshore VSM 735) from 300 to 900 K. Heat capacity measurements were made from 2 to 200 K using a commercial cryostat (PPMS9, Quantum Design). Neutron diffraction measurements were carried out from 10 to 300 K with a wavelength of λ=1.835 Å using high-resolution powder diffractometer (HRPD) at the Korea Atomic Energy Research Institute. All the diffraction data were analyzed using the FULLPROF program.[10]

III. RESULTS AND ANALYSIS

As shown in Fig. 1, all the x-ray diffraction patterns can be indexed according to the $P6_3cm$ space group and refined

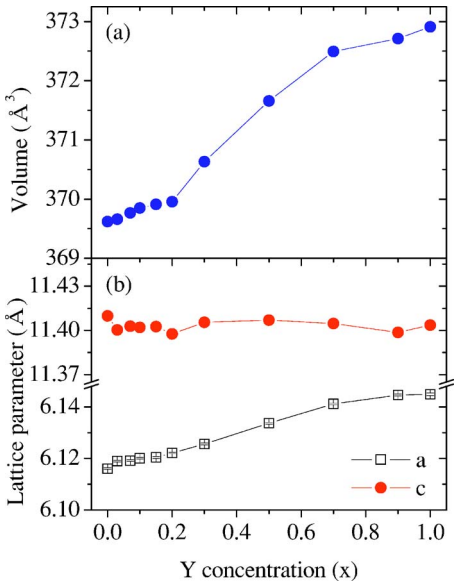

FIG. 2. (Color online) The lattice parameters and unit cell volume are shown as a function of Y concentration. Error bars are smaller than the symbol size.

using FULLPROF with reasonable agreement factors: for example, agreement factors of the final refinement were better than R_{wp}=4.8% and R_p=3.6% for all $Er_{1-x}Y_xMnO_3$. With increasing Y concentration, the c axis lattice constant remains almost unchanged while the a axis lattice constant expands from 6.116 to 6.145 Å, i.e., a total increase of about 0.5%. The unit cell volume increases too with increasing Y concentration, following roughly the Vegard law (see Fig. 2). Interestingly enough, all hexagonal manganites except for $ScMnO_3$ have more or less the same c axis lattice constant within 0.5% of one another while the a axis lattice constant varies by 1.6% altogether.

In order to study doping effects on the magnetic properties, we measured magnetization from 2 to 1000 K, which is shown in Fig. 3. First of all, we note that there is no clear anomaly at the antiferromagnetic transition temperature in the magnetization of all the samples. In fact, it is only clearly

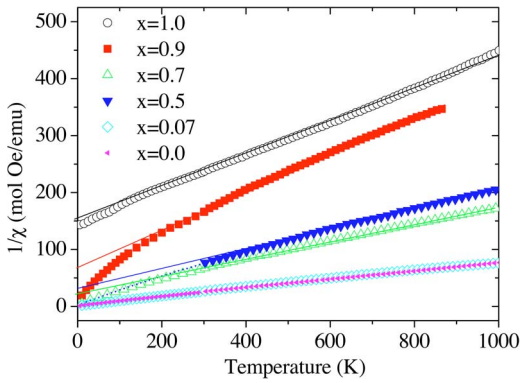

FIG. 3. (Color online) The temperature dependence of the inverse susceptibility is shown for six representative samples of $Er_{1-x}Y_xMnO_3$. All our measurements were made with applied field of 5 kOe. The line is for Curie-Weiss fit with the effective moment and the Curie-Weiss temperature shown in Fig. 5.

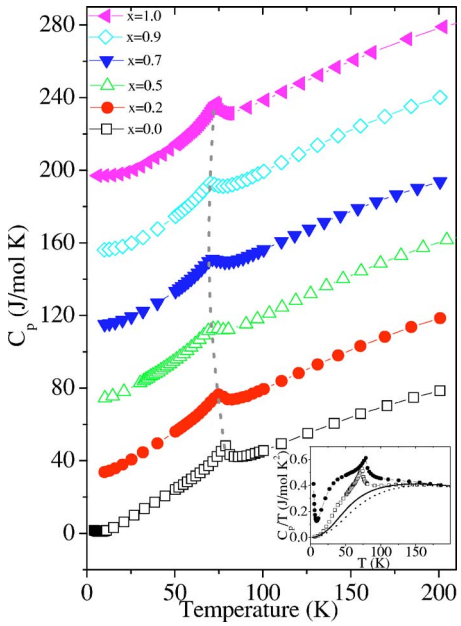

FIG. 4. (Color online) The temperature dependence of specific heat is shown for $Er_{1-x}Y_xMnO_3$. The data are shifted upwards for the sake of presentation. The curved dashed line indicates how the antiferromagnetic transition temperature evolves with doping. Temperature dependence of C_p/T of $ErMnO_3$ (solid circle) and $YMnO_3$ open square) is shown in the inset together with their respective phonon estimates: $ErMnO_3$ (solid line) and $YMnO_3$ (dashed line).

seen in the magnetization of single crystal samples.[11] Second, there is a very wide temperature range where the usual Curie-Weiss law is found to hold. Nevertheless, that the Curie-Weiss behavior is found mostly above 300 K warns one of danger in deducing the Curie-Weiss temperature of a hexagonal manganite from data taken only up to room temperature. The lines are for Curie-Weiss fit of the results; the estimated effective moments (μ_{eff}) and Curie-Weiss temperature (θ_{CW}) are shown in Fig. 5. Unmistakable doping effects found in Fig. 3 are that with increasing Er concentration θ_{CW} decreases continuously while μ_{eff} increases simultaneously.

As we cannot determine the antiferromagnetic transition temperature accurately enough from the susceptibility data shown in Fig. 3, we measured the heat capacity of six representative samples from 2 to 200 K. The data shown in Fig. 4 now display a clear peak structure indicative of the antiferromagnetic transition temperature. With increasing Er concentration, T_N initially drops before increasing continuously as shown by a dashed line in Fig. 4. We also plotted C/T for $YMnO_3$ and $ErMnO_3$ in the inset. As one can see, the peak structure is more pronounced in this plot with $ErMnO_3$ having a peak at higher temperature than $YMnO_3$. Apart from the peak at the antiferromagnetic transition, one can also see a conspicuous shoulder structure around 40 K and a sharp increase below 10 K in the plot for $ErMnO_3$. The low temperature upturn is likely to be due to Er moment ordering observed previously.[12] Regarding the shoulder structure seen in the $ErMnO_3$ data, we note that a similar, but weaker, structure is also observed for $YMnO_3$ as shown in the inset. For comparison, $LuMnO_3$ and $ScMnO_3$ show a similar feature, too.[13] Therefore, one possible explanation of the shoulder structure in $ErMnO_3$ is that it is an intrinsic effect closely associated with Mn moment ordering. An alternative explanation would be to ascribe it to an Schottky anomaly due to the splittings of Er crystal field levels. However, that a similar, albeit weaker, anomaly is found in $YMnO_3$, $LuMnO_3$, and $ScMnO_3$ goes against the explanation of the Schottky anomaly. Therefore, our present conclusion is that the shoulder structure is related to Mn moment ordering, which is somehow modified by its coupling with the Er moments.

In order to calculate magnetic entropy from the heat capacity data, we have estimated the phonon contribution using the Debye model with two Debye temperatures: for $YMnO_3$ (dashed line) we used $\theta_1=413\pm5$ K and $\theta_2=805\pm6$ K whereas we used $\theta_1=354\pm5$ K and $\theta_2=825\pm6$ K for $ErMnO_3$ (solid line). This two-Debye-temperature model can be rationalized by the fact that there are two kinds of elements in our samples: three relatively heavy elements (Y, Er, and Mn) and a relatively light element (O), which are expected to give rise to distinctively different Debye temperatures. We note that a similar model was used for the analysis of the heat capacity data for other hexagonal manganites with Debye temperatures in a similar range to ours.[13] By subtracting off the phonon contribution from the raw data, we have obtained the total magnetic entropy of 13.0 ± 2.0 J mol^{-1} K^{-1} for $YMnO_3$ and 23.5 ± 3.5 J mol^{-1} K^{-1} for $ErMnO_3$ at 200 K. It is very close to the theoretical value of the magnetic entropy (13.4 J mol^{-1} K^{-1}) for $YMnO_3$ while it is smaller than the theoretical value of the magnetic entropy (36.4 J mol^{-1} K^{-1}) for $ErMnO_3$. Unfortunately, however, we cannot separate out the magnetic entropy due to the Mn moments alone from the data obtained from the Er doped samples, because there are two Er sites in the hexagonal manganites whose crystal field splittings are not presently known.

We have plotted the Y concentration dependence of T_N and θ_{CW} in Fig. 5(a) and the frustration factor $f(=|\theta_{CW}|/T_N)$ in Fig. 5(b). As one can see, the frustration factor gets enhanced from 1.0 for $ErMnO_3$ to 4.8 for $Er_{0.1}Y_{0.9}MnO_3$ before increasing sharply to 7.8 for pure $YMnO_3$. The drastic increase of the frustration factor seen near $x=1.0$ is in sharp contrast with the rather smooth concentration dependence of the effective moment as shown in Fig. 5(c). For example, the effective moment decreases gradually from $\mu_{eff}=10.0\mu_B$ for $ErMnO_3$ to $\mu_{eff}=5.1\mu_B$ for $YMnO_3$: the error bar in the estimation of the ordered moment is smaller than $0.04\mu_B$ for all the concentrations. We note that the experimental values of μ_{eff} are in good agreement with our calculations using the following formula: $\mu_{eff}=[(1-x)^2\mu_{Er}{}^2+\mu_{Mn}{}^2]^{1/2}$, where $1-x$ is the Er concentration while μ_{Er} and μ_{Mn} are the effective magnetic moment of Er^{3+} ($\mu_{Er}=9.6\mu_B$) and Mn^{3+} ($\mu_{Mn}=4.9\mu_B$), respectively. Therefore, the data indicate that with increasing Er concentration the systems become less magnetically frustrated. One possible explanation we can think of is that, as Er ions sit in between two adjacent Mn planes with large frustration, the Er moments are bound to increase a magnetic coupling between the Mn moments at the $z=0$ and $z=1/2$ planes along the c axis. This increased magnetic coupling along the c axis then might as well reduce

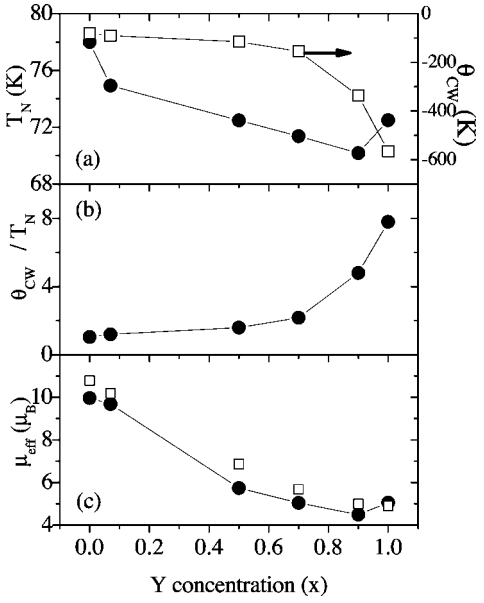

FIG. 5. We plot as a function of Y concentration (a) the Néel temperature (solid circle) and the Curie-Weiss temperature (open square), (b) the frustration parameter $f(=|\Theta_{CW}|T_N)$, and (c) μ_{eff} obtained from the bulk susceptibility (solid circle) and theoretically calculated value (open square) as discussed in the text. Error bars are smaller than the symbol size.

such frustration effects; how many moments and how they are magnetically coupled are the most important factors for geometrical frustration.

As we noted in the Introduction, our previous studies[6,7] of the magnetic structures of $YMnO_3$ and $ErMnO_3$ showed that the magnetic structure of $YMnO_3$ belongs to either Γ_1 or Γ_3 representation while that of $ErMnO_3$ belongs to either Γ_2 or Γ_4 representation with a zero c-axis component for both $YMnO_3$ and $ErMnO_3$. The evolution of the magnetic structure upon doping can be readily seen even in the raw data taken at 10 K (see Fig. 6). For example, the (1 0 0) Bragg peak is of purely magnetic origin and totally absent for

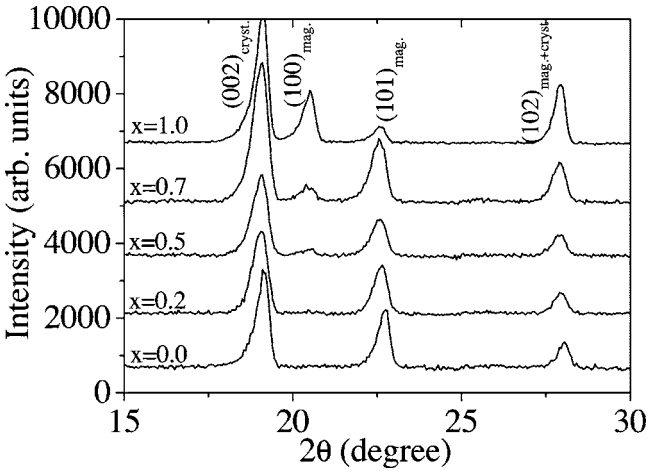

FIG. 6. The neutron diffraction patterns taken at 10 K are shown for $Er_{1-x}Y_xMnO$. The data are shifted upwards for better presentation.

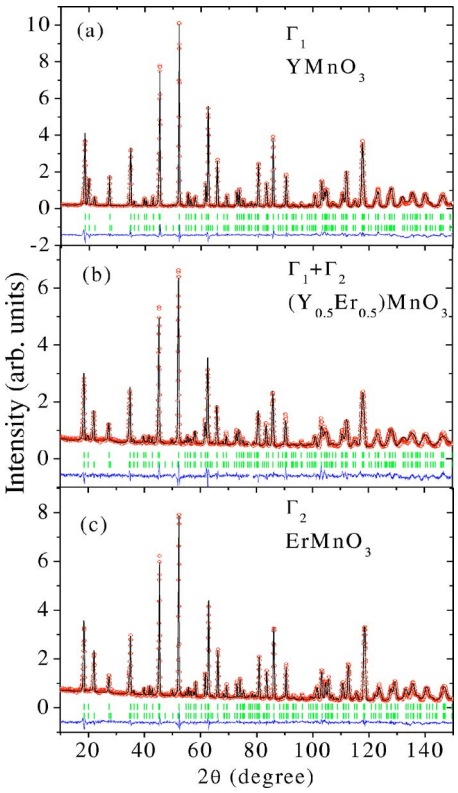

FIG. 7. (Color online) The observed (symbols) and calculated (line) neutron diffraction patterns for three representative $Er_{1-x}Y_xMnO_3$ samples, taken at 10 K. In order to refine the data, we used (a) the Γ_1 representation for $YMnO_3$, (b) the $\Gamma_1+\Gamma_2$ representations for $Er_{0.5}Y_{0.5}MnO_3$, and (c) the Γ_2 representation for $ErMnO_3$. The lines at the bottom of each figure are for the difference curve between the observed and calculated diffraction patterns. The first row of bars just below the data indicates the position of the nuclear Bragg peaks and the second row indicates the position of the magnetic Bragg peaks.

$ErMnO_3$ while another purely magnetic (1 0 1) peak is seen for both $YMnO_3$ and $ErMnO_3$. As one can see, the ratio of the intensity of the two magnetic peaks varies with increasing doping. The change in the ratio can be explained by mixing the two magnetic structures of $YMnO_3$ and $ErMnO_3$. Another equally viable model is that the two magnetic structures may exist inhomogeneously in space, i.e., magnetic phase separation.

In order to analyze the data, we first assumed that the true magnetic structure of $(Er_{1-x}Y_x)MnO_3$ is a mixed structure of the Γ_1 and Γ_2 representations with a zero c axis component as shown in Fig. 8(c).[14] The angle between the direction of the Mn moment at the Mn1 position and the [1 0 0] direction is denoted by Φ, i.e., $\Phi=90°$ for Γ_1 and $\Phi=0°$ for Γ_2. Typical refinement results taken at 10 K are shown in Fig. 7 for three representative samples. During the refinement of all the data, we achieved reasonable agreement factors for our fittings: for example, $R_B=4.8\%$, $R_f=5.2\%$, and $R_{mag}=10.1\%$ for $(Er_{0.5}Y_{0.5})MnO_3$, of which summary of the refinement results is given in Table I. We note that a model with mixed Γ_3 and Γ_4 representations is found to be equally good and gives more or less the same agreement factors.[15]

TABLE I. The summary of the refinement results of neutron powder diffraction patterns taken at 10 K for $Er_{0.5}Y_{0.5}MnO_3$. The space group is $P6_3cm$ and the model of the magnetic structure is mixed ($\Gamma_1+\Gamma_2$).

	Site	x	y	z
Er(1)	2*a*	0.000	0.000	0.285(2)
Er(2)	4*b*	1/3	2/3	0.240(2)
Y(1)	2*a*	0.000	0.000	0.285(2)
Y(2)	4*b*	1/3	2/3	0.240(2)
Mn	6*c*	0.339(21)	0.000	0.000
O(1)	6*c*	0.309(1)	0.000	0.166(2)
O(2)	6*c*	0.638(1)	0.000	0.341(2)
O(3)	2*a*	0.000	0.000	0.483(2)
O(4)	4*b*	1/3	2/3	0.024(2)

a=6.1106(2) Å $\quad \mu_{Mn}=3.08(3)\mu_B$
c=11.4020(5) Å $\quad$ Angle(Φ)=24.1(1)°
V=368.7(2) Å^3
χ^2=2.9
R_B=4.8%
R_f=5.2%
R_{mag}=10.1%

We plot Φ and μ_{ord}, obtained from refining the 10 K data, as a function of Y concentration in Fig. 8. As one can see, the angle Φ increases gradually upon doping from 0° for $ErMnO_3$ to 90° for $YMnO_3$. This variation of Φ is in sharp contrast with the observation that the ordered moment remains almost unchanged at $\mu_{ord}\simeq 3.2\mu_B$ and shows a very small doping dependence. For comparison, as Mn is in a 3^+ valence state all the way from $YMnO_3$ to $ErMnO_3$ it is expected to have a full spin moment of $4\mu_B$ under the assumption that the orbital moment is completely quenched. Therefore, there is about $0.8\mu_B$ of the Mn moments still fluctuating at 10 K for all the compositions.

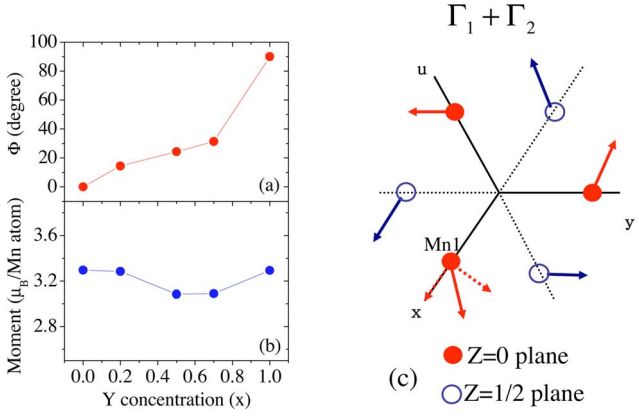

FIG. 8. (Color online) We show (a) the angle (Φ) between the direction of the Mn moment at the Mn1 position and the [1 0 0] axis and (b) the ordered magnetic moment of Mn, obtained from the refinement of the 10 K data, as a function of Y concentration. Error bars are smaller than the symbol size. (c) A schematic picture of the mixed magnetic structure ($\Gamma_1+\Gamma_2$), where the in-plane hexagonal axes are defined by $\mathbf{e}_x$, $\mathbf{e}_y$, and $\mathbf{e}_u=-(\mathbf{e}_x+\mathbf{e}_y)$.

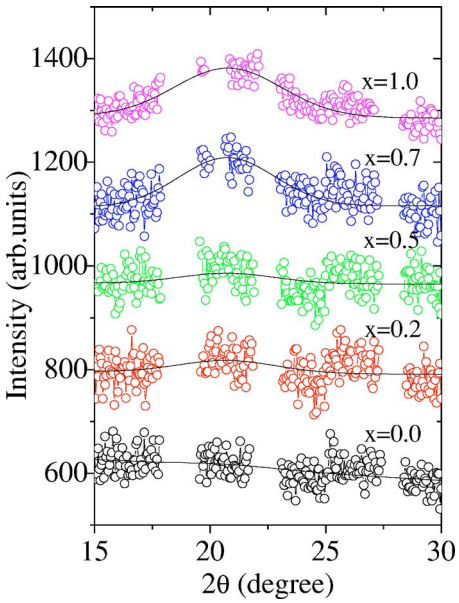

FIG. 9. (Color online) The magnetic diffuse scattering taken at 65 K is shown for five samples of $Er_{1-x}Y_xMnO_3$ after removing Bragg peaks. The lines are for Gaussian curve fitting results. The data are shifted upwards for better presentation.

As regards the question of fluctuating Mn moments, it is interesting to see how diffuse scattering previously seen for $YMnO_3$ in Ref. 9 changes upon doping. As in $YMnO_3$, there is clear evidence of diffuse scattering in the 2θ range of 15° to 30° for doped samples. Nevertheless, it is also noticeable that the intensity of the diffuse scattering becomes gradually weakened with increasing Er concentration. There is a particularly pronounced change in the intensity of the diffuse scattering between x=0.7 and x=0.5. Within the resolutions of our experiments, there is hardly any diffuse scattering for pure $ErMnO_3$ as shown in Fig. 9. The doping dependence of the diffuse scattering appears to be consistent with that of the frustration factor, f, as shown in Fig. 5(b).

IV. DISCUSSION

As we noted in the previous sections, systems with a triangular spin structure are naturally expected to have geometrical frustration effects. Despite that $YMnO_3$ and $ErMnO_3$ both have similar 2D triangular spin structures, however, experimental evidence of such frustration effects is very different from one to another. Although $YMnO_3$ shows all the signs of Mn moments being frustrated, such signs are almost absent for $ErMnO_3$. For example, $ErMnO_3$ shows a very weak signature of diffuse scattering and a much smaller frustration parameter, f, compared with that of $YMnO_3$ although both $YMnO_3$ and $ErMnO_3$ have about the same ordered moments of $3.2\mu_B$ at 10 K. Our doping experiments demonstrate that this disparate frustrating effect ought to be closely related to the presence of the Er moments. As shown in the doping dependence of both frustration parameter and

diffuse scattering, even a small amount of Er doping turns out to be very detrimental to geometrical frustration effects. We rule out a possibility that our data are simply masked by strong magnetic signals from Er. Experimental evidence against this possibility is that we observed the strong doping dependence in the frustration parameter in spite of the gradual and natural doping dependence of the effective moments as shown in Fig. 5(c). Furthermore, the diffuse scattering significantly reduced upon Er doping is additional evidence supporting our conclusion that the frustration effects of the Mn moments are greatly affected by Er doping. Related to the drastic doping effects, it is interesting to note that a layer of Er ions is situated between two Mn layers that are magnetically coupled along the *c* axis. Thus we think that it is quite probable that a magnetic coupling between the Er and Mn moments relieves the frustration effects inherent to the 2D Mn moment ordering.

To summarize, we have found that Er doping at the Y site of $YMnO_3$ significantly modifies the geometrical frustration effects of the Mn moments with a triangular spin structure. We suggest that a magnetic coupling between the Er and Mn moments plays an important role here. Another important result is that the magnetic structures of $YMnO_3$ and $ErMnO_3$ are found to become easily mixed upon doping and evolve from one state to another continuously without a sign of abrupt change.

ACKNOWLEDGMENTS

We thank A. Pirogov for helpful discussions and the Korea Basic Science Institute for allowing us to use a heat capacity setup. Work at SungKyunKwan University was supported by the CNRF project of Ministry of Science and Technology and the Center for Strongly Correlated Materials Research.

*Author to whom correspondence should be addressed. Email address: jgpark@skku.edu

[1] M. A. Gilleo, Acta Crystallogr. **10**, 161 (1957).
[2] H. Yakel, W. C. Koehler, E. F. Bertaut, and F. Forrat, Acta Crystallogr. **16**, 957 (1963).
[3] I. G. Ismailzade and S. A. Kizhaev, Sov. Phys. Solid State **7**, 236 (1965); G. Smolenskii and I. Chupis, Sov. Phys. Usp. **25**, 475 (1982).
[4] E. F. Bertaut and M. Mercier, Phys. Lett. **5**, 27 (1963).
[5] A. Munoz, J. A. Alonso, M. J. Martinez-Lope, M. T. Casais, J. L. Martinez, and M. T. Fernandez-Diaz, Phys. Rev. B **62**, 9498 (2000).
[6] J. Park, U. Kong, A. Pirogov, S. I. Choi, J.-G. Park, Y. N. Choi, C. Lee, and W. Jo, Appl. Phys. A: Mater. Sci. Process. **A74**, S796 (2002).
[7] J. Park, U. Kong, S. I. Choi, J.-G. Park, C. Lee, and W. Jo, Appl. Phys. A: Mater. Sci. Process. **A74**, S802 (2002).
[8] A. P. Ramirez, in *Handbook of Magnetic Materials*, edited by K. H. J. Buschow (North-Holland, Amsterdam, 2001), Vol. 13.
[9] Junghwan Park, J.-G. Park, Gun Sang Jeon, Han-Yong Choi, Changhee Lee, W. Jo, R. Bewley, K. A. McEwen, and T. G. Perring, Phys. Rev. B **68**, 104426 (2003).
[10] J. Rodríguez-Carvajal, Physica B **192**, 55 (1993).
[11] For example, one can compare the magnetization data of single crystal and polycrystal $YMnO_3$ prepared by the same group: T. Katsufji, S. Mori, M. Masaki, Y. Moritomo, N. Yamamoto, and H. Takagi, Phys. Rev. B **64**, 104419 (2001); **66**, 134434 (2002).
[12] M. Fiebig, C. Degenhardt, and R. V. Pisarev, Phys. Rev. Lett. **88**, 027203 (2002).
[13] D. G. Tomuta, S. Ramakrishnan, G. J. Nieuwenhuys, and J. A. Mydosh, J. Phys.: Condens. Matter **13**, 4543 (2001).
[14] Using the basis vectors given in Ref. 5, we constructed a model of the mixed structure as a linear combination of the basis vectors of the Γ_1 and Γ_2 representation. Thus in our model for a given composition the three Mn moments at the $z=0$ plane are rotated by the same amount of the angle Φ in the same sense from the [1 0 0] direction, and the same thing goes for the three Mn moments at the $z=1/2$ plane.
[15] Instead of the mixed structure described in the text, we have also tried to analyze the data using two representations of Γ_1 and Γ_2 as separate phases, i.e., a magnetically phase separated model, to find that this model is also equally good. Since such a phase separation phenomenon is often observed in orthorhombic manganites upon doping, it is plausible that there may well be a magnetic phase separation in the hexagonal manganites, which requires further investigation.